Physica E 124 (2020) 114358

Contents lists available at ScienceDirect

Physica E: Low-dimensional Systems and Nanostructures

journal homepage: http://www.elsevier.com/locate/physe

Janus Ga_2STe monolayer under strain and electric field: Theoretical prediction of electronic and optical properties

Hong T.T. Nguyen [a,b], Vo T.T. Vi [c], Tuan V. Vu [a,b], Huynh V. Phuc [d], Chuong V. Nguyen [e], Hien D. Tong [f], Le T. Hoa [g,h,*], Nguyen N. Hieu [g,h]

[a] Division of Computational Physics, Institute for Computational Science, Ton Duc Thang University, Ho Chi Minh City, Viet Nam
[b] Faculty of Electrical & Electronics Engineering, Ton Duc Thang University, Ho Chi Minh City, Viet Nam
[c] Department of Physics, University of Education, Hue University, Hue, Viet Nam
[d] Division of Theoretical Physics, Dong Thap University, Dong Thap, Viet Nam
[e] Department of Materials Science and Engineering, Le Quy Don Technical University, Ha Noi, Viet Nam
[f] Faculty of Engineering, Vietnamese–German University, Binh Duong, Viet Nam
[g] Institute of Research and Development, Duy Tan University, Da Nang 550000, Viet Nam
[h] Faculty of Natural Sciences, Duy Tan University, Da Nang 550000, Viet Nam

ARTICLE INFO

Keywords:
Janus Ga2STe monolayer
Electronic structures and optical properties
Strain engineering and electric field
DFT calculations

ABSTRACT

In this work, detailed investigations of the electronic and optical properties of a Janus Ga_2STe monolayer under a biaxial strain and electric field have been performed using density functional theory. Via the phonon spectrum and ab-initio molecular dynamics simulations, the dynamical and thermal stabilities of the Janus Ga_2STe monolayer are verified. Our obtained results showed that the Janus Ga_2STe exhibits a direct semiconducting characteristic and its band gap depends greatly on the biaxial strain. While both the electronic and optical properties are very weakly dependent on the electric field, strain engineering can cause a direct–indirect band gap transitions in the Janus Ga_2STe. At equilibrium, the optical absorbance of the Janus Ga_2STe monolayer is activated in the infrared light region of about 0.9 eV, which is close to its band gap value. The main peak of the optical absorbance spectrum is located in the ultraviolet light region with an absorbance intensity of 11.914×10^4 cm^{-1} may be increased by compression strain. In particular, the absorbance intensity of the Janus Ga_2STe monolayer increases rapidly in the visible light region, reaching 4.810×10^4 cm^{-1} and can be altered by strain. Our results not only show that the Janus Ga_2STe monolayer has many promising applications in opto-electronic devices but also motivates experimental works on Janus structures in near future.

1. Introduction

After the experimental exploration of graphene successfully [1], a wide-ranging search of two-dimensional (2D) layered nanomaterials took place shortly thereafter. 2D nanomaterials have shown themselves to be potential objects for applications in electronics and optoelectronics with outstanding chemical and physical properties that are not possible in bulk materials [2–7]. Many 2D layered nanomaterials have been experimentally synthesized recently, such as silicene [8], stenene [9], transition metal dichalcogenide monolayers [10], monochalcogenides [11,12]. Among them, with a wide natural band gap, monochalcogenides are predicted to be promising candidates for applications in photocatalytic water splitting and energy storage devices [7,13,14]. Particularly, the monochalcogenide group III monolayers [15] have attracted the attention of the scientific community because they possess many interesting physical properties, such as very high carrier mobility or good on/off ratio, which are necessary for applications in field-effect transistors [16–18].

Recently, a new kind of 2D layered nanomaterials, Janus structures of transition metal dichalcogenides have been successfully synthesized by experiments [19,20]. The asymmetric out-of-plane geometric structure of the Janus MoSSe has been confirmed [19], which is different from the mirror symmetry structure of MoS_2. It is well-known that the geometric symmetry plays a decisive role in defining the electronic properties of 2D layered nanomaterials. The breaking of the mirror symmetry structure in the Janus materials gives them many new

* Corresponding author. Institute of Research and Development, Duy Tan University, Da Nang 550000, Viet Nam.
E-mail addresses: nguyenthithamhong@tdtu.edu.vn (H.T.T. Nguyen), vuvantuan@tdtu.edu.vn (T.V. Vu), lethihoa8@duytan.edu.vn (L.T. Hoa), hieunn@duytan.edu.vn (N.N. Hieu).

https://doi.org/10.1016/j.physe.2020.114358
Received 29 April 2020; Accepted 9 July 2020
Available online 25 July 2020

properties compared to the original material MoS_2. The successfully experimental synthesis of the Janus MoSSe monolayer from MoS_2 is an important milestone, with the meaning of finding a new member for the 2D family. It provides additional motivation for the studies of other Janus structures, which can be formed from dichalcogenides or monochalcogenides. Accordingly, the Janus structures of dichalcogenides were extensively studied by density functional theory (DFT) [21–24]. They showed that the electronic properties of the Janus structures can be driven by a strain engineering [24] or electrostatic gating [21]. Yang and co-workers demonstrated that the absorption intensity of the Janus MoSeTe is up to 1×10^6 cm^{-1} which is suitable for optoelectronic applications [25]. Recently, Janus structures of monochalcogenides, especially Janus group-III monochalcogenides, have received particular attention because they have outstanding chemical and physical properties as promising candidates for optoelectronic and photocatalytic applications [26–28]. Also, heterostructures based on 2D Janus structures have been theoretically predicted to have interesting physical properties with great potential for applications [29–31].

Motivated by the above-mentioned outstanding properties and promising applications of Janus structures, electronic structures and optical properties of the Janus Ga_2STe monolayer under a biaxial strain and electric field are systematically considered using density functional theory in this work. The dynamical and thermal stabilities of the Janus structure have been checked first. We focus on the influence of the strain and electric field on the band structures, band gap, and basic optical characteristics of the Janus Ga_2STe monolayer. The prospect of controlling band gap and optical absorbance of the Janus Ga_2STe monolayer by strain or electric field has also been carefully investigated in this work.

2. Computational details

In this study, the calculations were based on density functional theory (DFT) using the Quantum Espresso package [32]. We used the generalized gradient approximations (GGA) of Perdew-Burke-Ernzerhof (PBE) functional [33,34] to consider the exchange-correlation interaction. A $(15 \times 15 \times 1)$ *k*-mesh in the Brillouin zone was adopted for the Janus structure. The cut-off energy for the plane-wave basis is set to be 500 eV. All computed structures, including the cell parameters and atom positions, were fully optimized. The criteria for the force during relaxation was 10^{-3} eV/Å and the energy convergence criteria between consecutive steps was 10^{-6} eV. We used a vacuum space of 20 Å perpendicularly to the 2D monolayer surface to avoid artificial interactions that may exist between periodic images of slabs along the vertical direction. Also, the Heyd–Scuseria–Ernzerhof (HSE06) hybrid functional [35] is also used to obtain more accurate the band gap of monolayers at equilibrium. Furthermore, to check the dynamical and thermal stabilities of the Janus Ga_2STe monolayer at room temperature, the phonon spectrum and ab-initio molecular dynamics (AIMD) simulations are also performed in this study.

3. Results and discussion

The Janus monochalcogenide monolayer Ga_2STe monolayer can be constructed from GaTe or GaSe monolayer by replacing one layer of Te (S) atoms in GaTe (GaS) monolayer with S(Te) atoms. At equilibrium, the GaTe and GaS monolayers belong to the symmetry group $P\bar{6}m2$ (D_{3h}) with mirror symmetry. This mirror symmetry will be broken when the Janus structure of Ga_2STe is formed and it belongs to the symmetric group *P*3*m*1 (C_{3v}) without out-plane mirror symmetry. The geometrical symmetry and structural perfection in 2D layered nanomaterials are important characteristics for defining electronic properties. Atomic structure after fully relaxation of the Janus Ga_2STe monolayer are depicted in Fig. 1(a). Our calculations demonstrate that the lattice constant of the Janus monochalcogenide Ga_2STe monolayer is a = 3.899 Å. Compared to the GaS and GaTe monolayers, the lattice constant of the Janus Ga_2STe is larger than that of the GaS monolayer but smaller than that of the GaTe monolayer. However, as listed in Table 1, we can see that the Ga–Ga bond lengths in all three monolayers are almost the same. Also, charge density of the atoms in the Janus Ga_2STe monolayer is depicted in Fig. 1(b and c). We can see that the electron density is enriched around the Ga and Te atoms meanwhile the charge density around the S atom is quite low.

To improve the dynamical and thermal stabilities, the phonon spectrum and AIMD simulation for the Janus Ga_2STe monolayer have been performed as depicted in Fig. 2. As shown in Fig. 2(a), the phonon spectrum of the Janus Ga_2STe monolayer has 12 vibrational modes including three acoustic modes and nine optical modes. There are no negative frequencies in the phonon dispersion curves of the Janus Ga_2STe monolayer. It implies that the Janus Ga_2STe monolayer is dynamically stable at equilibrium. To verify the thermal stability of the Janus Ga_2SeTe monolayer, we perform the AIMD simulations for the temperature fluctuation within 6000 time steps (6 ps). Snapshots of atomic structures of the Janus Ga_2STe before and after heating 6 ps and the time-dependence of temperature fluctuation of the Janus Ga_2SeTe monolayer by AIMD simulations are depicted in Fig. 2(b). We can see that the geometrical structure of the Janus Ga_2STe monolayer is still robust and only slightly distortion after heat treatment within 6 ps at a temperature of 300 K by AIMD simulations. There are no structural reconstruction and bond breaking in the Janus Ga_2SeTe monolayer at room temperature, confirming its thermal stability at room temperature.

As depicted in Fig. 3, Janus Ga_2STe monolayer at equilibrium exhibits a semiconducting characteristic with a direct band gap which is different from both GaTe and GaS, which are indirect semiconductors [15]. We all know that the PBE calculations underestimate the energy-gap of the insulators and semiconductors [36] and HSE06 calculations can obtain more accurate results. As illustrated in Fig. 3, the obtained band structures by the HSE06 and PBE methods are the same profile. Our calculations demonstrate that the band gap of the Janus Ga_2STe monolayer is 0.912 eV and 1.549 eV at the PBE and HSE06 levels. The energy gap of the Janus Ga_2STe monolayer is much smaller than that of both GaS and GaTe monolayer as listed in Table 1. Our results are consistent with the previous DFT calculations [27,28] The direct gap of the Janus Ga_2STe monolayer is located at the Γ-point in the first Brillouin zone. Concentrating on the contribution of atomic orbitals to the formation of electronic bands, we plotted out the partial density of states of electrons as presented also in Fig. 3. We can see that the valence band of the Janus monolayer is strongly donated by the S-*p* and T-*p* orbitals. The S-*s*, T-*s*, and Ga-*d* orbitals contribute insignificantly to the formation of electronic bands, especially the valence band. Also, the internal charge distribution of constituent atoms in the Janus Ga_2STe monolayer has been calculated by Mulliken population analysis [37] as listed in Table 2. Our calculations demonstrate that there is a difference in charge between Ga atoms in two different layers in the Janus Ga_2STe structure. The charge of gallium atom, which is connected with S (Ga_S), is much larger than that of the Ga_{Te}.

As mentioned above, electron states and optical characteristics of 2D layered nanomaterials are very sensitive to structural perfection and geometrical structure. The breaking of the mirror symmetry in Janus Ga_2STe structure made its electronic properties different from those of GaS or GaTe monolayer. In this part, we take into account the influence of a biaxial strain ϵ_b on the electronic properties of the Janus Ga_2STe monolayer. To quantitatively estimate the effects of the biaxial strain, we define the biaxial strain ϵ_b via the lattice constants of the monolayer before strain λ_0 and after strain λ as: $\epsilon_b = (\lambda - \lambda_0)/\lambda_0$. Negative and positive values of the ϵ_b refer to the monolayer under compressive and tensile strains, respectively. Band structures of the Janus Ga_2STe monolayer under different values of the biaxial strain ϵ_b are depicted in Fig. 4. Our obtained results demonstrate that while the conduction band is greatly affected by the compressive strain, the tensile strain has significantly changed the valence band. Especially the strains have

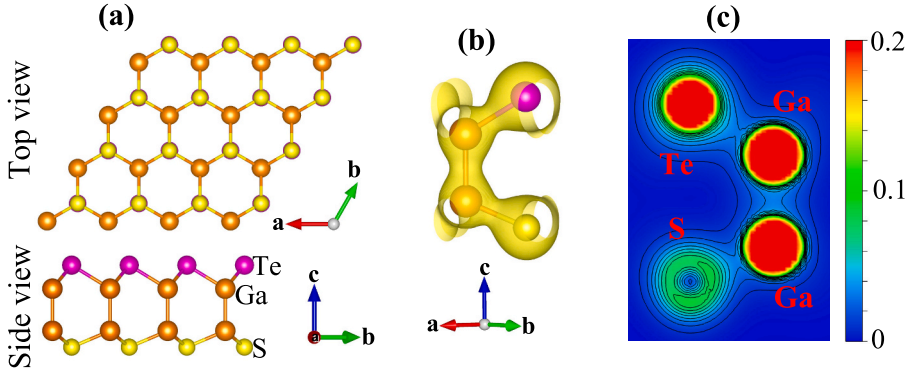

Fig. 1. Janus Ga_2STe monolayer at equilibrium: (a) Optimized geometrical structure in different views, (b) charge density with isolated 0.04, and (c) contour plot of the electron density from 0 to 0.2e Bohr^{-3} with the interval of 0.02 Bohr^3.

Table 1
The lattice constant a, the bond lengths d, thickness h, and the calculated band gaps at the PBE E_g^{PBE} and HSE06 E_g^{HSE06} levels.

	a (Å)	d_{Ga-S} (Å)	d_{Ga-Te} (Å)	d_{Ga-Ga} (Å)	h (Å)	E_g^{PBE} (eV)	E_g^{HSE} (eV)
GaS	3.585	2.471	–	2.457	4.651	2.586	3.312
GaTe	4.084	–	2.683	2.454	5.004	1.411	2.137
Ga_2STe	3.899	2.446	2.639	2.468	4.802	0.912	1.549

changed the positions of the conduction band minimum (CBM) when $\epsilon_b < 0$ and the valence band maximum (VBM) when $\epsilon_b > 0$. In the case of compressive strain as shown in Fig. 4(a), it is clearly seen that the compressive strain not only reduces the band gap of the Janus Ga_2STe monolayer but also tends to cause the CBM to shift from the Γ-point to the M-point. The consequence of this is that the indirect–direct band gap transition has been found at $\epsilon_b = -6\%$. Similarly, the indirect–direct band gap transition has been also found in the Janus Ga_2STe monolayer in the presence of the tensile strain as shown in Fig. 4(b). However, unlike the case of compressive strain, the tensile strain caused the VMB to move from the Γ-point to the point located on the ΓM-path while the CMB was still at the Γ-point. Compared to the case of strain engineering, our calculations indicate that the electronic properties of the Janus Ga_2STe monolayer are weakly influenced by the electric field. Fig. 5 presents the band structure of the Janus Ga_2STe monolayer in the presence of an electric field. In presence of electric field, the Janus structure Ga_2STe was still a direct semiconductor. The energy gap is weakly changed due to the applied electric field. Band gaps of the Ga_2STe as functions of the biaxial strain ϵ_b and electric field E are presented in Fig. 6. We can see that the band gap of the Ga_2STe decreases in the presence of compressive strain. However, this decrease in the band gap is quite slow in the range from 0 to −5%. This is also the strain interval where the Janus Ga_2STe monolayer retains the direct semiconducting characteristic. The band gap of the Janus monolayer decreases rapidly as we continue to increase the compressive strain, and within this strain interval, from −6% to −10%, the Janus Ga_2STe monolayer exhibits indirect semiconducting characteristic. In the case of tensile strain, the Janus Ga_2STe monolayer is exhibited to be a direct semiconductor in the tensile strain range from 0 to 7%, and its band gap is increased in this strain range. As the strain continued to increase, its band gap suddenly decreased and the direct semiconducting characteristic the Janus Ga_2STe monolayer was replaced by the indirect semiconducting characteristic. In the presence of an electric field, the band gap of the Janus Ga_2STe monolayer decreases linearly with the increasing of the electric field as illustrated in Fig. 6(b). However, the effect of the electric field on the band gap is quite weak. In a large range of electric fields, the band gap of the Janus Ga_2STe monolayer only decreases by 14%, from 0.912 eV at E = 0–0.785 eV at E = 5 V/nm.

In the last part, we investigate the optical properties of the Janus Ga_2STe monolayer when the biaxial strain ϵ_b and electric field E are individually applied. The incident light is parallel polarized (along the a-axis) with energy ranging from 0 eV to 10 eV. It is well-known that the basic optical properties can be calculated via the dielectric constant, which is defined by $\epsilon(\omega) = \epsilon_1(\omega) + i\epsilon_2(\omega)$. The imaginary part $\epsilon_2(\omega)$ can be obtained first by the sum of the transitions between filled and unfilled states and the real part $\epsilon_1(\omega)$ is then derived from the Kramer–Kronig relation [38,39]:

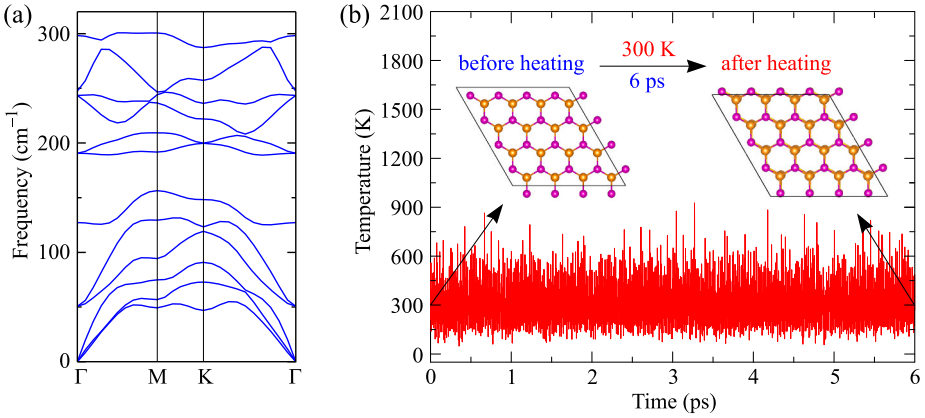

Fig. 2. (a) Phonon spectrum of the Janus Ga_2STe at equilibrium. b) Ab initio molecular dynamics calculation of temperature fluctuation of the Janus Ga_2SeTe monolayer as a function of time at room temperature. Insets are the AIMD snapshots for the Janus Ga_2SeTe monolayer before and after heating.

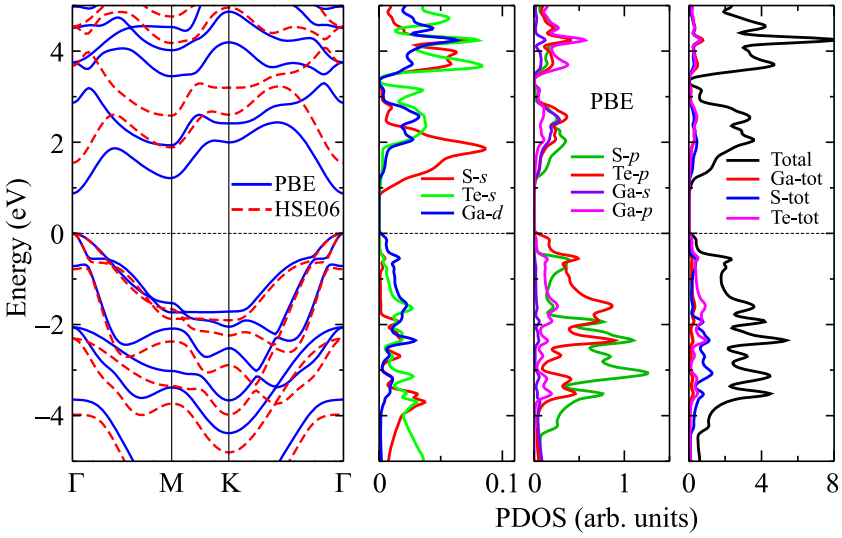

Fig. 3. Band structure and PDOS of the Janus Ga_2STe monolayer at equilibrium.

Table 2
Internal charge distribution (e) of constituent atoms in the Janus Ga_2STe monolayer. $Ga_{S/Te}$ stands for the Ga atom connected to S/Te atom.

	s	*p*	*d*	Total	Charge
Ga_{Te}	1.12	1.74	10	12.85	0.15
Ga_S	1.304	1.34	10	12.65	0.35
S	1.88	4.55	0	6.43	−0.43
Te	1.91	4.16	0	6.07	−0.07

$$\epsilon_2^{ij}(\omega) = \frac{4\pi^2 e^2}{Vm^2\varpi^2}\sum_{nn'\sigma}\langle kn\sigma|p_i|kn'\sigma\rangle\langle kn'\sigma|p_j|kn\sigma\rangle \times f_{kn}(1-f_{kn'})\delta(E_{kn'}-E_{kn}-\hbar\omega) \quad (1)$$

and

$$\epsilon_1(\omega) = 1 + \frac{2}{\pi}P\int_0^\infty \frac{\omega'\epsilon_2(\omega')}{\omega'^2-\omega^2}d\omega', \quad (2)$$

where e and m are the electron charge and electron mass, respectively, ω is the angular frequency of the incident light, V is the volume of the unit-

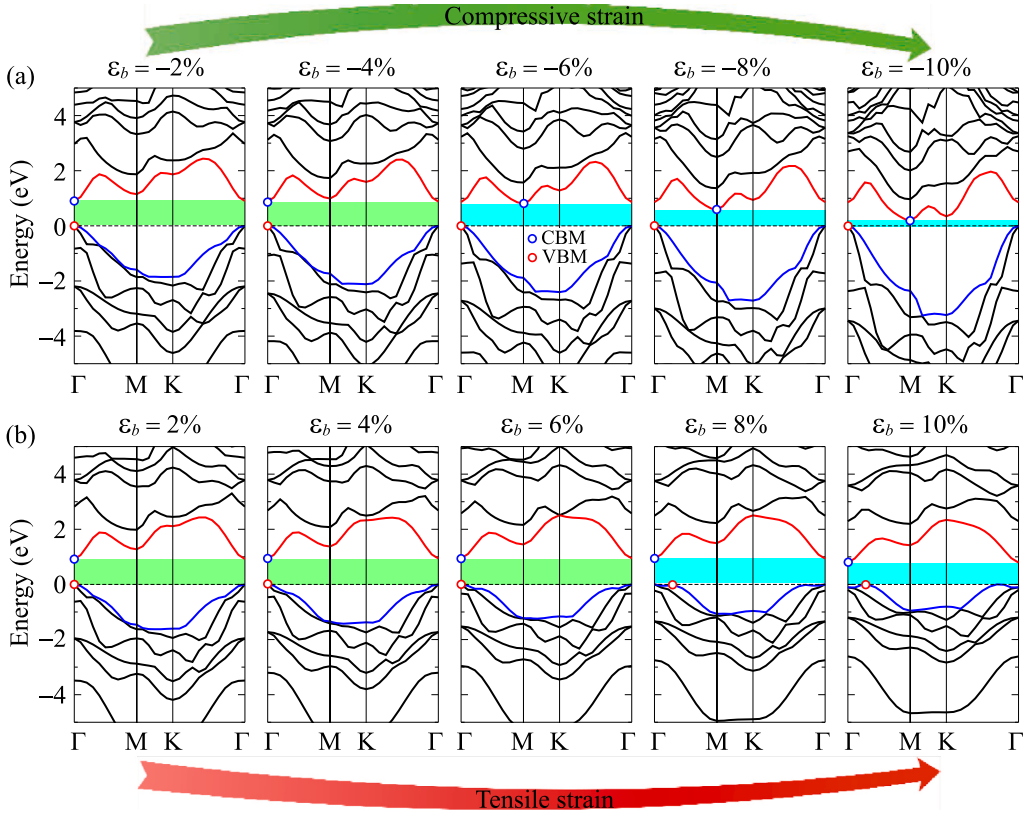

Fig. 4. Calculated band structures of the Ga_2STe under (a) compressive and (b) tensile strains using the PBE functional.

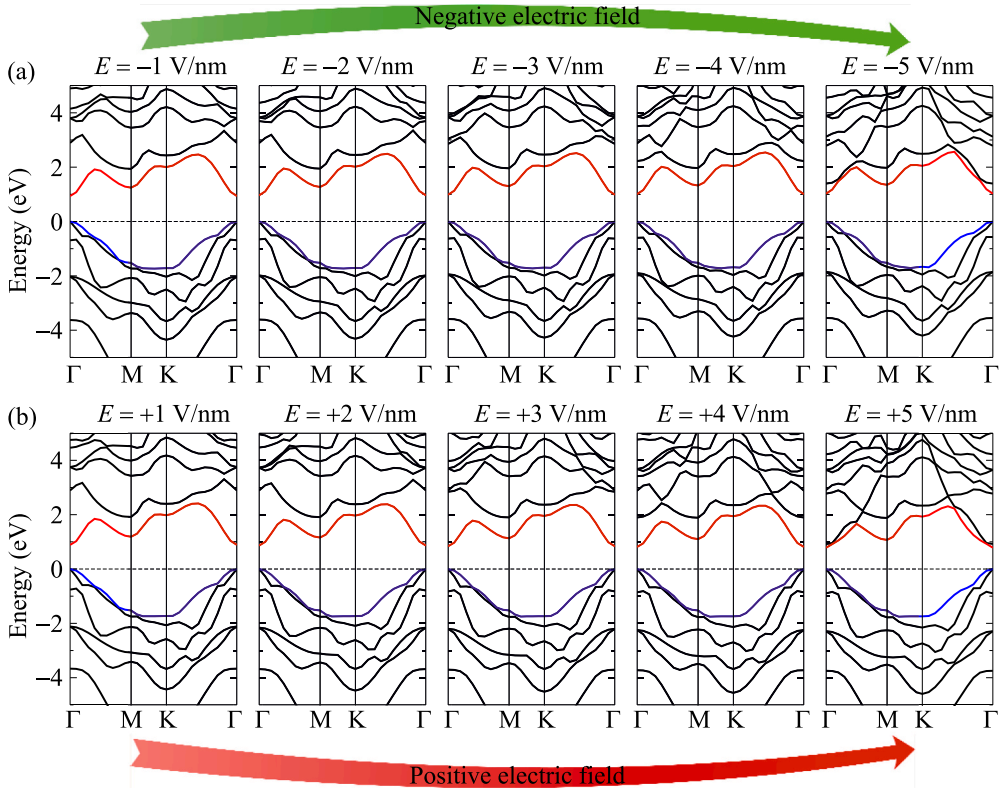

Fig. 5. Band structures of the Ga_2SeTe under (a) negative and (b) positive electric field.

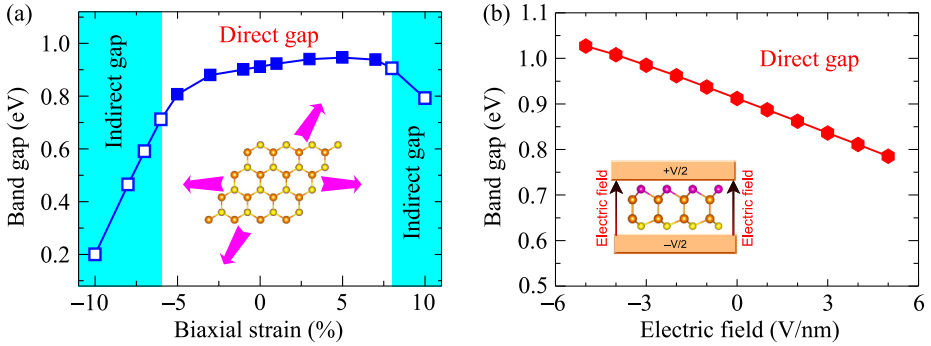

Fig. 6. Band gap of Ga_2STe as a function of a biaxial strain ϵ_b (a) and external electric field E (b). Filled and open shapes refers to the direct and indirect gaps, respectively.

cell, p is the momentum operator, $|knp\rangle$ is the crystal wave-function, and f_{kn} is the Fermi distribution function.

Calculated the dielectric function parts of the Janus Ga_2STe monolayer under the strain engineering ϵ_b and electric field E are presented in Fig. 7. It is well-known that, in the Penn model [40], the static dielectric constant $\epsilon_1(0)$ is inversely proportional to the direct energy gap of the materials. Our obtained results indicate that the static dielectric constant of the Janus Ga_2STe monolayer is $\epsilon_1(0) = 3.863$. While the effects of the E on the spectra of the $\epsilon(\omega)$ can be ignored as illustrated in Fig. 7 (b), the dielectric function of the Janus Ga_2STe monolayer depends strongly on the strain engineering as shown in Fig. 7(a). We focus on the spectrum of the imaginary part $\epsilon_2(\omega)$ which is tightly connected the optical characteristics of the semiconductors. We can see that the main peak in the spectrum of the $\epsilon_2(\omega)$ locates at the incident light energy of 3.80 eV. The compressive strain causes this peak to shift to a higher energy region while it will move to a lower energy region in the presence of tensile strain.

The optical absorbance spectrum $A(\omega)$ and optical reflectivity $R(\omega)$, which can be derived from the $\epsilon(\omega)$, are expressed as [41]:

$$A^{ij}(\omega) = \frac{\sqrt{2}\omega}{c}\left[\sqrt{\epsilon_1^{ij}(\omega)^2 + \epsilon_2^{ij}(\omega)^2} - \epsilon_1^{ij}(\omega)\right]^{1/2} \tag{3}$$

and

$$R^{ij}(\omega) = \left|\frac{\sqrt{\epsilon_1^{ij}(\omega) + i\epsilon_2^{ij}(\omega)} - 1}{\sqrt{\epsilon_1^{ij}(\omega) + i\epsilon_2^{ij}(\omega)} + 1}\right|^2. \tag{4}$$

The influence of the ϵ_B and electric field E on the optical absorbance spectrum $A(\omega)$ and reflectivity $R(\omega)$ is depicted in Fig. 8. At equilibrium, the optical absorbance of the Janus Ga_2STe monolayer is activated in the infrared light region of about 0.9 eV, which is close to its band gap value. The main peak of the optical absorbance spectrum $A(\omega)$ is located at the incident light energy of 6.127 eV with an absorbance intensity of 11.914 $\times 10^4$ cm^{-1}. Similar to the spectrum of the dielectric function as above-

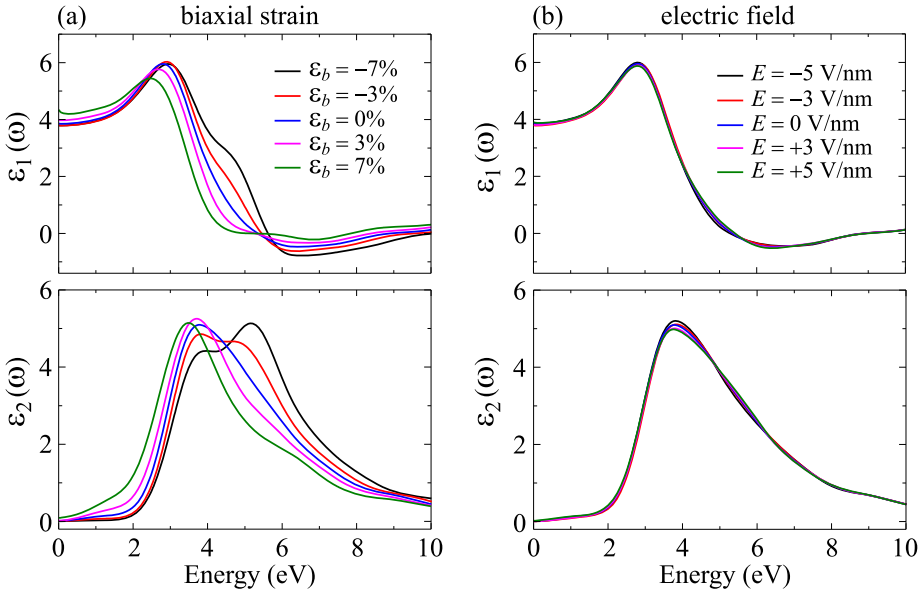

Fig. 7. The real $\epsilon_1(\omega)$ and imaginary $\epsilon_2(\omega)$ parts of the dielectric function for the Ga_2STe under different levels of (a) biaxial strain ϵ_b and (b) electric field E.

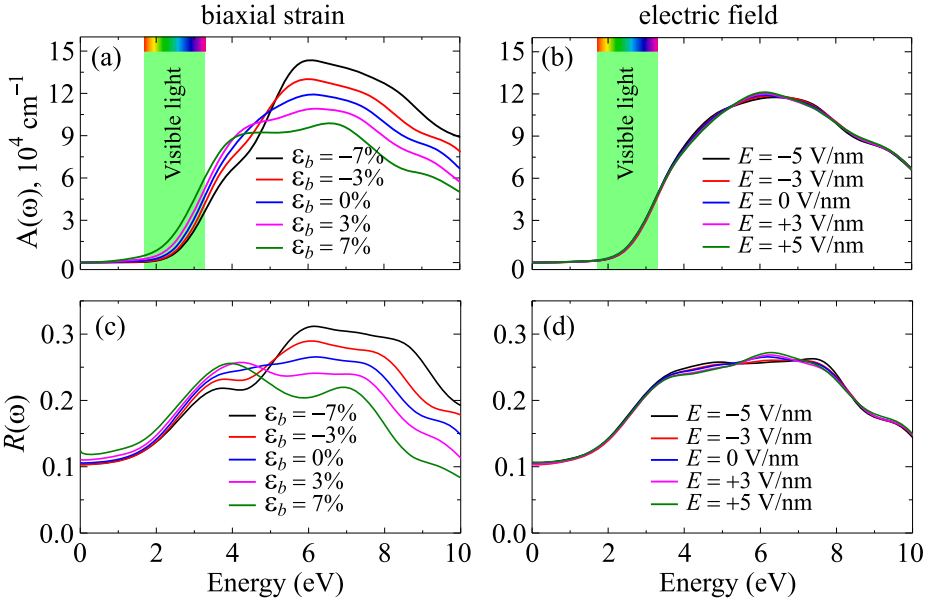

Fig. 8. The optical absorbance spectra $A(\omega)$ (a,b) and optical reflectivity $R(\omega)$ (c,d) for the Ga_2STe under the biaxial strain and electric field.

mentioned, the effect of the electric field on other optical spectra such as the absorption coefficient [Fig. 8(b)] and optical reflectivity [Fig. 8(d)] is negligible. Meanwhile, the $A(\omega)$ can be strongly altered by the biaxial strain ϵ_b as illustrated in Fig. 8(a). The maximum absorption intensity is in the ultraviolet light region and may be increased by compression strain. At the same time, the compressive strain also causes the main absorption peak to shift slightly to the lower energy region. Absorption intensity increases quite quickly in the visible light region, reaching 4.810×10^4 cm^{-1} and can be altered by strain although the change in the absorption intensity due to strain is not large. Similar to the absorption spectrum, the effect of distortion on optical reflectivity is evident in the ultraviolet light region with photon energy higher than 5 eV.

4. Conclusion

In the present study, we systematically considered the electronic and optical properties of the Janus Ga_2STe monolayer in the presence of the biaxial strain and electric field. Our calculations for phonon dispersion curves and AIMD simulations proved that the Janus Ga_2STe monolayer is dynamical and thermal stabilities at room temperature and can physically exist. The mirror symmetry breaking in the Janus structure leads to the Janus Ga_2STe monolayer possessing many new properties, which do not exist in GaS or GaTe monolayers. The Janus Ga_2STe monolayer has a broad absorption spectrum, which extends from the infrared to the ultraviolet light region, and it has a high absorption intensity in the visible light region. The sensitivity of electron states and optical properties of the Ga_2STe to strain, especially the occurrence of the direct–indirect gap transitions due to strain and high absorption intensity, can turn the Janus Ga_2STe monolayer becoming an excellent

nanomaterial for applications in optoelectronic devices.

Declaration of competing interest

I declare that I have no significant competing financial, professional, or personal interests that might have influenced the performance or presentation of the work described in this manuscript.

Acknowledgments

This work was supported by the Domestic Master/PhD Scholarship Programme of Vingroup Innovation Foundation.

References

[1] K.S. Novoselov, A.K. Geim, S.V. Morozov, D. Jiang, Y. Zhang, S.V. Dubonos, I. V. Grigorieva, A.A. Firsov, Science 306 (2004) 666.
[2] M. Xu, T. Liang, M. Shi, H. Chen, Chem. Rev. 113 (2013) 3766.
[3] Z. Hu, Y. Ding, X. Hu, W. Zhou, X. Yu, S. Zhang, Nanotechnology 30 (2019) 252001.
[4] K.D. Pham, N.N. Hieu, H.V. Phuc, I.A. Fedorov, C.A. Duque, B. Amin, C.V. Nguyen, Appl. Phys. Lett. 113 (2018) 171605.
[5] N.D. Hien, C.V. Nguyen, N.N. Hieu, S.S. Kubakaddi, C.A. Duque, M.E. Mora-Ramos, L. Dinh, T.N. Bich, H.V. Phuc, Phys. Rev. B 101 (2020), 045424.
[6] C.V. Nguyen, N.N. Hieu, N.A. Poklonski, V.V. Ilyasov, L. Dinh, T.C. Phong, L. V. Tung, H.V. Phuc, Phys. Rev. B 96 (2017) 125411.
[7] H.L. Zhuang, R.G. Hennig, Chem. Mater. 25 (2013) 3232.
[8] B. Lalmi, H. Oughaddou, H. Enriquez, A. Kara, S. Vizzini, B. Ealet, B. Aufray, Appl. Phys. Lett. 97 (2010) 223109.
[9] F.-f. Zhu, W.-j. Chen, Y. Xu, C.-l. Gao, D.-d. Guan, C.-h. Liu, D. Qian, S.-C. Zhang, J.-f. Jia, Nat. Mater. 14 (2015) 1020.
[10] G. Deokar, D. Vignaud, R. Arenal, P. Louette, J.-F. Colomer, Nanotechnology 27 (2016), 075604.
[11] S. Acharya, M. Dutta, S. Sarkar, D. Basak, S. Chakraborty, N. Pradhan, Chem. Mater. 24 (2012) 1779.
[12] D.D. Vaughn, R.J. Patel, M.A. Hickner, R.E. Schaak, J. Am. Chem. Soc. 132 (2010) 15170.
[13] Y. Zhou, M. Zhao, Z.W. Chen, X.M. Shi, Q. Jiang, Phys. Chem. Chem. Phys. 20 (2018) 30290.
[14] G. Shi, E. Kioupakis, Nano Lett. 15 (2015) 6926.
[15] S. Demirci, N. Avazli, E. Durgun, S. Cahangirov, Phys. Rev. B 95 (2017) 115409.
[16] D.A. Bandurin, A.V. Tyurnina, G.L. Yu, A. Mishchenko, V. Zólyomi, S.V. Morozov, R.K. Kumar, R.V. Gorbachev, Z.R. Kudrynskyi, S. Pezzini, Z.D. Kovalyuk, U. Zeitler, K.S. Novoselov, A. Patanè, L. Eaves, I.V. Grigorieva, V.I. Falko, A.K. Geim, Y. Cao, Nat. Nanotechnol. 12 (2017) 223.
[17] D.J. Late, B. Liu, J. Luo, A. Yan, H.S.S.R. Matte, M. Grayson, C.N.R. Rao, V. P. Dravid, Adv. Mater. 24 (2012) 3549.
[18] S. Sucharitakul, N.J. Goble, U.R. Kumar, R. Sankar, Z.A. Bogorad, F.-C. Chou, Y.-T. Chen, X.P.A. Gao, Nano Lett. 15 (2015) 3815.
[19] A.-Y. Lu, H. Zhu, J. Xiao, C.-P. Chuu, Y. Han, M.-H. Chiu, C.-C. Cheng, C.-W. Yang, K.-H. Wei, Y. Yang, Y. Wang, D. Sokaras, D. Nordlund, P. Yang, D.A. Muller, M.-Y. Chou, X. Zhang, L.-J. Li, Nat. Nanotechnol. 12 (2017) 744.
[20] J. Zhang, S. Jia, I. Kholmanov, L. Dong, D. Er, W. Chen, H. Guo, Z. Jin, V.B. Shenoy, L. Shi, J. Lou, ACS Nano 11 (2017) 8192.
[21] Y. Sun, Z. Shuai, D. Wang, Nanoscale 10 (2018) 21629.
[22] T.V. Vu, H.D. Tong, D.P. Tran, N.T.T. Binh, C.V. Nguyen, H.V. Phuc, H.M. Do, N. N. Hieu, RSC Adv. 9 (2019) 41058.
[23] W. Shi, Z. Wang, J. Phys. Condens. Matter 30 (2018) 215301.
[24] J. Yuan, Y. Shan, T. Li, J. Phys. D Appl. Phys. 53 (2020) 125502.
[25] X. Yang, D. Singh, Z. Xu, Z. Wang, R. Ahuja, J. Mater. Chem. C 7 (2019) 12312.
[26] L. Hu, D. Wei, J. Phys. Chem. C 122 (2018) 27795.
[27] A. Huang, W. Shi, Z. Wang, J. Phys. Chem. C 123 (2019) 11388.
[28] Y. Guo, S. Zhou, Y. Bai, J. Zhao, Appl. Phys. Lett. 110 (2017) 163102.
[29] T.V. Vu, N.V. Hieu, H.V. Phuc, N.N. Hieu, H. Bui, M. Idrees, B. Amin, C.V. Nguyen, Appl. Surf. Sci. 507 (2020) 145036.
[30] W. Zhou, Z. Yang, A. Li, M. Long, F. Ouyang, Phys. Rev. B 101 (2020), 045113.
[31] D.D. Vo, T.V. Vu, N.V. Hieu, N.N. Hieu, H.V. Phuc, N.T.T. Binh, L.T.T. Phuong, M. Idrees, B. Amin, C.V. Nguyen, Phys. Chem. Chem. Phys. 21 (2019) 25849.
[32] P. Giannozzi, S. Baroni, N. Bonini, M. Calandra, R. Car, C. Cavazzoni, D. Ceresoli, G.L. Chiarotti, M. Cococcioni, I. Dabo, A.D. Corso, S. de Gironcoli, S. Fabris, G. Fratesi, R. Gebauer, U. Gerstmann, C. Gougoussis, A. Kokalj, M. Lazzeri, L. Martin-Samos, N. Marzari, F. Mauri, R. Mazzarello, S. Paolini, A. Pasquarello, L. Paulatto, C. Sbraccia, S. Scandolo, G. Sclauzero, A.P. Seitsonen, A. Smogunov, P. Umari, R.M. Wentzcovitch, J. Phys. Condens. Matter 21 (2009) 395502.
[33] J.P. Perdew, K. Burke, M. Ernzerhof, Phys. Rev. Lett. 77 (1996) 3865.
[34] J.P. Perdew, K. Burke, M. Ernzerhof, Phys. Rev. Lett. 78 (1997) 1396.
[35] J. Heyd, G.E. Scuseria, M. Ernzerhof, J. Chem. Phys. 118 (2003) 8207.
[36] J.P. Perdew, M. Levy, Phys. Rev. Lett. 51 (1983) 1884.
[37] R.S. Mulliken, J. Chem. Phys. 23 (1955) 1833.
[38] A. Delin, P. Ravindran, O. Eriksson, J. Wills, Int. J. Quant. Chem. 69 (1998) 349.
[39] S.Z. Karazhanov, P. Ravindran, A. Kjekshus, H. Fjellvag, B.G. Svensson, Phys. Rev. B 75 (2007) 155104.
[40] D.R. Penn, Phys. Rev. 128 (1962) 2093.
[41] P. Ravindran, A. Delin, B. Johansson, O. Eriksson, J.M. Wills, Phys. Rev. B 59 (1999) 1776.